SEMARAK ILMU PUBLISHING

CFD Letters

Journal homepage:
https://semarakilmu.com.my/journals/index.php/CFD_Letters/index
ISSN: 2180-1363

Effects of Operating Conditions on Evaporation Rate and Wall Shear Stress Development in a Micro-gap Heat Sink with Internal Micro-Fins

Shugata Ahmed[1], Erwin Sulaeman[2,*], Ahmad Faris Ismail[2], Muhammad Hasibul Hasan[3], Zahir Hanouf[4]

[1] Department of Robotics and Mechatronics Engineering, Faculty of Engineering and Technology, University of Dhaka, Dhaka 1000, Bangladesh
[2] Department of Mechanical Engineering, Faculty of Engineering, International Islamic University Malaysia, Jalan Gombak, 53100 Kuala Lumpur, Malaysia
[3] Departmental of Mechanical and Industrial Engineering, Faculty of Engineering and Architectural Science, Ryerson University, 350 Victoria Street, Toronto, ON 5MB 2K3, Canada
[4] Department of Mechanical Engineering, Faculty of Engineering. University of Bahrain, Bahrain

ARTICLE INFO

Article history:
Received 10 December 2021
Received in revised form 15 January 2022
Accepted 16 January 2022
Available online 24 February 2022

Keywords:
Micro-gap heat sink; micro-fins; wall heat flux; pumping power; void fraction

ABSTRACT

Evaporation in the micro-gap heat sink has a very high heat transfer coefficient. As a result, it is significant for high heat flux management. Heat transfer rate can be enhanced further by including internal micro-fins. However, the pressure drop penalty due to the small gap height and fin surfaces is a major concern. Wall shear stress development is responsible for pressure drop. This paper investigates the effects of operating conditions, e.g., wall heat flux, pumping power, and inlet void fraction, on evaporation rate and wall shear stress development in a micro-gap heat sink with internal micro-fins of rectangular and triangular profiles, while the cross-sectional area (21.8 mm^2) is kept constant. R-134a is considered as coolant. Results show that the evaporation rate from per unit volume increases with the increment of wall heat flux and decreases with the enhancement of pumping power. However, after a threshold value of the pumping power (2×10^{-4} W), the decrement rate falls. Again, the wall shear stress rises with the increasing wall heat flux and pumping power while reduces for escalating inlet void fraction.

1. Introduction

Micro-gap heat sinks have potentials to serve as high performance coolant flow paths [1]. Alam *et al.,* [2] showed that for high heat flux and low mass flow rate, micro-gaps have higher heat transfer capability compared to microchannel heat sinks. Heat transfer rate can be enhanced further by including micro-fins in the micro-gap [3-7]. It has been reported that evaporation of the coolant in a micro-gap heat sink is efficient for cooling of electronic devices, micro-electromechanical systems (MEMS), micro-opto-electronic devices, and micro-reactors [8]. However, pressure drop is a major concern for micro-gaps due to the small gap height [9]. Wall shear stress development is responsible

* *Corresponding author.*
E-mail address: esulaeman@iium.edu.my (Erwin Sulaeman)

https://doi.org/10.37934/cfdl.14.2.19

for pressure drop in the heat sink [10]. Hence, it is important to investigate the effects of operating conditions on evaporation rate and wall shear stress.

This paper presents a numerical work to investigate the effects of operating conditions, e.g., wall heat flux, pumping power, and inlet void fraction, on evaporation rate and wall shear stress development in a micro-gap heat sink with rectangular and triangular fins for the R-134a coolant. Fluent solver in the Ansys 14.5 release has been used for the simulation purpose.

2. Simulation

2.1. Multiphase Flow and Turbulence Modelling

The Volume of Fluid (VOF) method [11] has been used to model the multiphase flow. The void fraction equation is the following:

$$\frac{\partial(\alpha\rho_v)}{\partial t} + \nabla.(\alpha\rho_v\vec{v}_v) = m_{evp} \tag{1}$$

Here α is the void fraction, ρ_v is the vapor density, $\vec{v}_v$ is the vapor velocity vector and m_{evp} is rate of mass transfer from liquid to vapor phase due to evaporation. The void fraction is defined mathematically as follows:

$$\alpha = \frac{1}{V}\int_V I(\chi,t)dV \tag{2}$$

Here $I(\chi,t)$ is known as the marker function, which is a multi-dimensional unit step function. In the primary phase, the value of the marker function is 1, while in the secondary phase it is 0.

The conservation of momentum equation:

$$\frac{\partial(\rho\vec{v})}{\partial t} + \nabla.(\alpha\rho\vec{v}\vec{v}) = -\nabla P + \nabla\tau + \rho\vec{g} + \vec{F} \tag{3}$$

Here τ is wall shear stress and g is gravitational acceleration. For Newtonian fluid, the shear stress is expressed as follows:

$$\tau = \mu[\nabla v + (\nabla v)T] \tag{4}$$

Here μ is the dynamic viscosity. The conservation of energy equation for the fluid domain:

$$\frac{\partial(\rho E)}{\partial t} + \nabla.\left(\vec{v}(\rho E + P)\right) = \nabla\left(k_{eff}\nabla T\right) \tag{5}$$

Here k_{eff} is the effective thermal conductivity. Again, for the solid domain:

$$\nabla.(k_s\nabla T_s) = \frac{\partial\left(\rho_s c_{p,s} T_s\right)}{\partial t} \tag{6}$$

Here $c_{p,s}$ is specific heat capacity of solid at constant pressure.

Internal fins are responsible for turbulence generation [8]. Hence, it is important to model turbulence in the flow field. The following equation is used to calculate the turbulence kinetic energy [12]:

$$\frac{\partial k}{\partial t} + \nabla(\vec{v}\,.\,k) = \frac{1}{\rho}[\nabla(a_k.\mu_{eff}.\nabla k) + G_k + G_b - \rho\varepsilon - Y_M + S_k] \quad (7)$$

Here, G_k = generation of turbulent kinetic energy due to the mean velocity gradients. G_b = generation of turbulent kinetic energy due to buoyancy. Y_M = contribution of the fluctuating dilatation in compressible turbulence to the overall dissipation rate. ε=turbulence energy dissipation rate.

Again, the equation based on turbulence kinetic energy dissipation rate:

$$\frac{\partial \varepsilon}{\partial t} + \nabla(\vec{v}\,.\,\varepsilon) = \frac{1}{\rho}[\nabla(a_\varepsilon.\mu_{eff}.\nabla\varepsilon) + C_{1\varepsilon}\frac{\varepsilon}{k}(G_k + C_{3\varepsilon}G_b) - C_{2\varepsilon}\rho\frac{\varepsilon^2}{k} - R_\varepsilon + S_\varepsilon] \quad (8)$$

α_k and α_ε are inverse effective Prandtl numbers for k and ε, respectively and S_k and S_ε are source terms.

The model constants have the following default values:
$C_{1\varepsilon}$= 1.42, $C_{2\varepsilon}$= 1.68

2.2 Modelling Mass Transfer

During boiling, mass is transferred from liquid to vapor phase. Modelling mass transfer rate due to evaporation includes determining empirical model for calculating evaporation rate and define the constraint to maintain interfacial temperature condition.

2.2.1 Interfacial temperature condition

Interface temperature condition is critical. According to Schrage [13], at thermodynamic equilibrium condition, a temperature jump at the interface exists due to pressure difference between vapour and bulk fluid. Hence, temperature condition at the interface can be written as: $T_{sat}(P_l)$=T_l≠T_v=$T_{sat}(P_v)$. To employ this condition in the mathematical model is a challenge.

2.2.2 Evaporation-condensation model

Mass exchange between two phases is calculated from evaporation-condensation model, proposed by Lee [14]. Following equation is used:

$$m_{evp} = coeff.(1-\alpha)\rho_l(T_l - T_{sat})T_{sat} \quad (9)$$

In this equation, the value of evaporation coefficient should be defined to maintain saturation temperature (T_{sat}) at the interface. Wu *et al.,* [15], De Schepper *et al.,* [16], and Alizadehdakhel *et al.,* [17] recommended that the value of evaporation coefficient should be 0.1 to satisfy the criterion.

2.3 Initial and Boundary Conditions

At time t = 0; v = 0, $T_f = T_s = T_{atm}$, α = 0. Various boundary conditions are defined at the inlet, outlet, and outer walls of the heat sinks. At the inlet: $T_f = T_{in}$, $v = v_{in}$, $\alpha = \alpha_{in}$. Turbulence intensity is also defined at the inlet. For fully developed internal flow, turbulence intensity is calculated from the following formula:

$$I = \frac{u'}{u_{avg}} = 0.16(Re)^{-\frac{1}{8}} \tag{10}$$

Again, atmospheric pressure is defined at the outlet: $P = P_{out}=P_{atm}$.

Heat transfer from wall to fluid is by convection. Convective heat transfer coefficient is calculated from the following equation:

$$h = \frac{Q_{eff}}{A_f(T_s - T)} \tag{11}$$

Uniform heat flux is applied at the bottom of the heat sink. Heat is transferred through the solid wall by conduction in the normal direction of the bottom surface. Heat flux transferred by conduction is calculated from the following equation:

$$q = -k_s \frac{\partial T_s}{\partial n} \tag{12}$$

Adiabatic condition is applied to other channel walls. Hence, q_{loss} = 0. As a result, temperature gradient at boundaries:

$$\frac{\partial T_s}{\partial n} = 0 \tag{13}$$

2.4 Heat-Sink Dimensions and Range of Operating Conditions

Dimensions of the micro-gap heat sink are shown in Table 1 and the range of operating conditions are given in Table 2. R-134a has been considered as coolant.

Table 1
Dimensions of micro-gap heat sinks

Parameters (unit)	Rectangular fin gap	Triangular fin gap
Cross-sectional area, A_{cs} *(mm^2)*	21.8	21.8
Convective surface area, A_f *(mm^2)*	2.66×10^{-3}	2.04×10^{-3}
Hydraulic diameter, D_h *(mm)*	1.11	1.45

Table 2
Range of operating conditions

Operating conditions (unit)	Range
Wall heat flux *(Wm^{-2})*	1×10^{6} - 8×10^{6}
Pumping power *(W)*	0.8×10^{-4} - 1×10^{-3}
Inlet void fraction	0 – 0.8

2.5 Validation of Numerical Model

The numerical model has been validated experimentally. The experimental setup has been presented in other publications of the author [6, 7]. Validation results are given in Figure 1 and Figure 2. Figure 1 shows that Biot number decreases with the increment of Reynolds number calculated from outlet vapour velocity. Pressure drop also decreases with the decrement of vapour Reynolds number (Figure 2). Note that in the figures, dimensionless heat flux is constant, which is the ratio of heat flux absorbed by the fluid to heat flux supplied at the bottom of the heat sink. Mathematically, $\bar{q} = \frac{q_{eff}}{q_{in}}$.

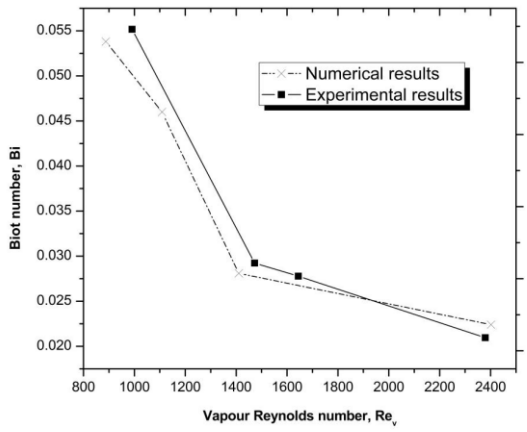

Fig. 1. Plot of Biot number against vapour Reynolds number for numerical and experimental results when $\bar{q}$=1

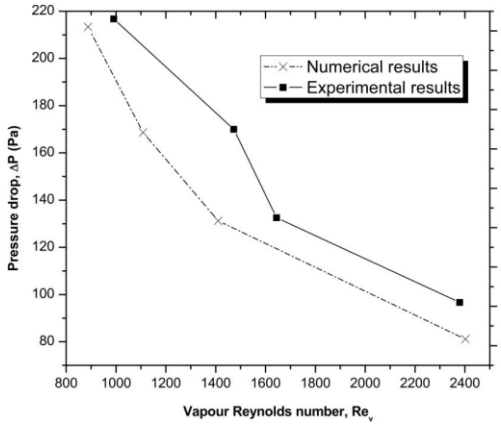

Fig. 2. Pressure drop vs. vapour Reynolds number plot for numerical and experimental results when $\bar{q}$=1

3. Results and Discussion

3.1 Evaporation Rate

Mass exchange from liquid to vapor phase is calculated from Eq. (9). From the equation, it is apprehended that evaporation rate depends on liquid superheat (T_l - T_{sat}), and void fraction (α). In Figure 3 and Figure 4, rate of mass transfer from per unit volume of fluid ($\dot{m}$) due to evaporation in rectangular and triangular-fin micro-gaps have been plotted for incrementing wall heat flux (q'') and pumping power (Ω). It is accomplished that rate of evaporation escalates with ascending heat flux. For a fixed saturation temperature, liquid superheat increases for increasing heat flux, which in turn augments evaporation rate. However, for advancing pumping power, a steeply decreasing trend of evaporation rate is noted at the beginning, which diminishes after surpassing 2×10^{-4} W of pumping power for both heat sinks (Figure 4).

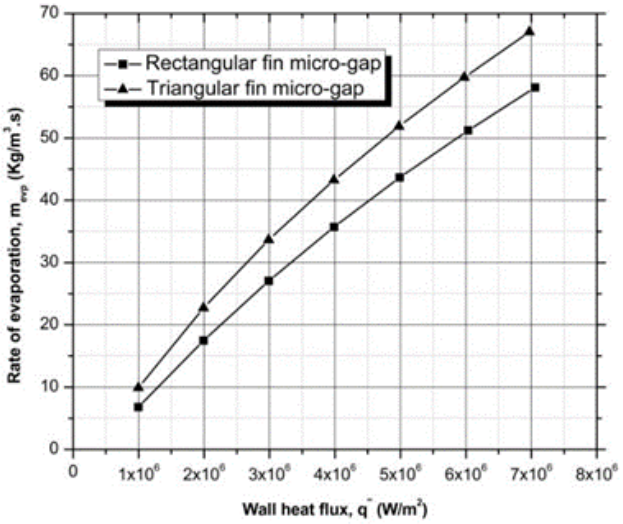

Fig. 3. Rate of evaporation from per unit volume for wall heat flux variation at Ω=3×10^{-3} W, α_{in}=0

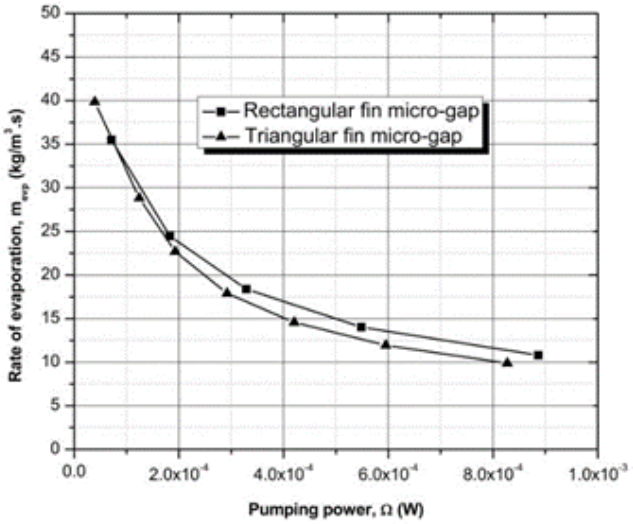

Fig. 4. Rate of evaporation from per unit volume for pumping power variation at q_{in}=1×10^6 Wm^{-2}, α_{in}=0

Due to ascending evaporation rate, total thermal resistance (R_{th}) increases with the increment of wall heat flux (Figure 5). Again, R_{th} decreases with the augmenting pumping power (Figure 6).

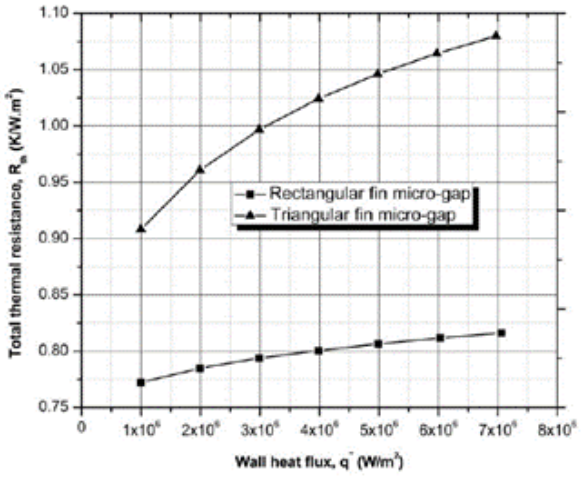

Fig. 5. Variation of total thermal resistance with wall heat flux (Ω=3×10^{-3} W, α_{in}=0)

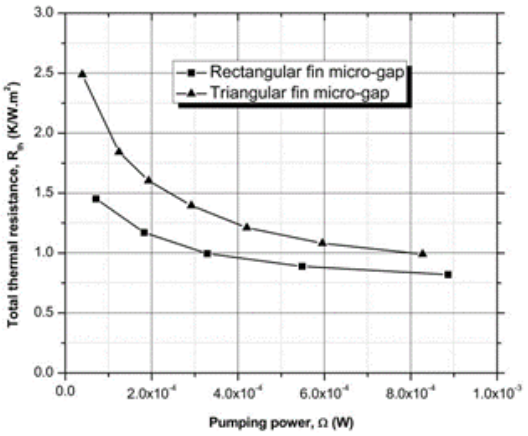

Fig. 6. Variation of total thermal resistance with pumping power (q_{in}=1×10^6 Wm^{-2}, α_{in}=0)

3.2 Wall Shear Stress Development

Wall shear stresses developed on upper and lower surfaces of rectangular and triangular fin micro-gaps during flow boiling have been plotted against heat flux, pumping power and inlet void fraction increment. It is seen that the wall shear stress increases with upgrading heat flux (Figure 7) and pumping power (Figure 8) in both heat sinks and decreases with rising inlet void fraction (Figure 9).

Wall shear stress development on lower surfaces of rectangular and triangular fin micro-gaps is visualized in Figure 10 and Figure 11, respectively. Almost uniform shear stress distribution on interfaces is noted. A slight variation can be perceived near walls of the heat sinks.

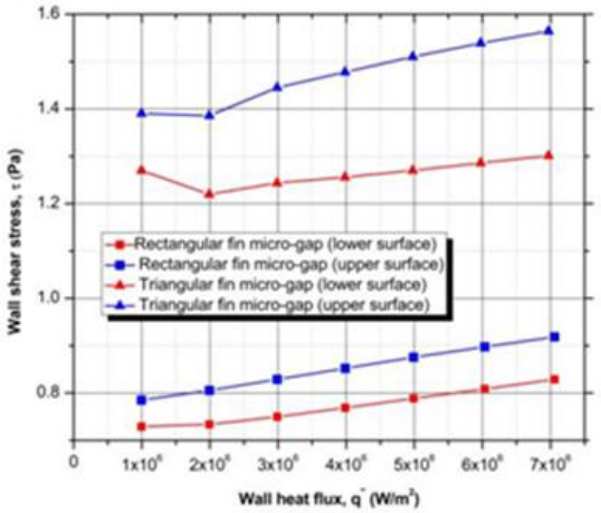

Fig. 7. Variation of the wall shear stress with the wall heat flux ($\Omega=3\times10^{-3}$ W, $\alpha_{in}=0$)

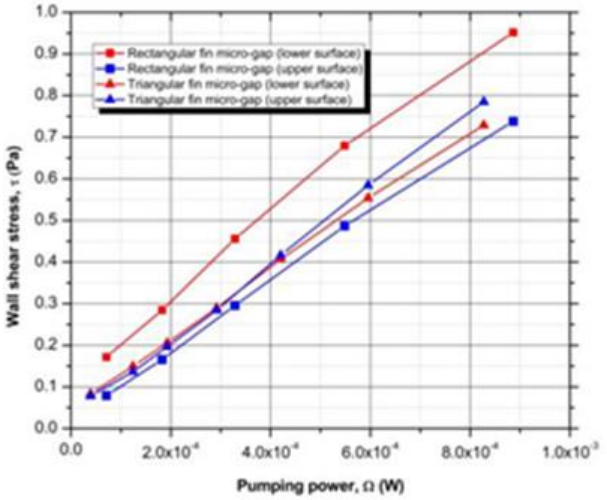

Fig. 8. Variation of the wall shear stress with the pumping power (qin=1×106 Wm-2, αin=0)

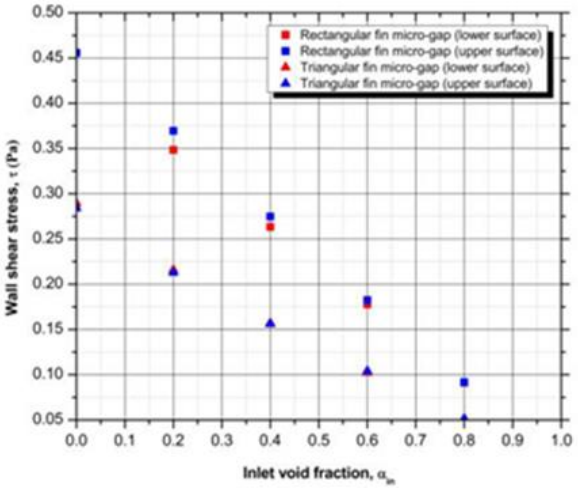

Fig. 9. Variation of the wall heat flux with the inlet void fraction ($\Omega=5.5\times10^{-4}$W, $q_{in}=1\times10^{6}$ Wm^{-2})

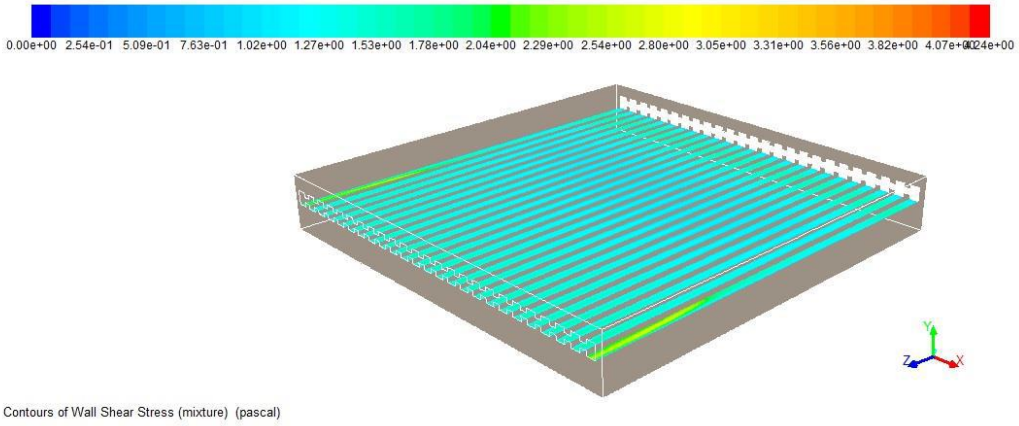

Fig. 10. Wall shear stress distribution on lower interface of a rectangular fin micro-gap for $\Omega=2\times10^{-3}W$, $q_{in}=1\times10^{6}\ Wm^{-2}$, $\alpha_{in}=0$

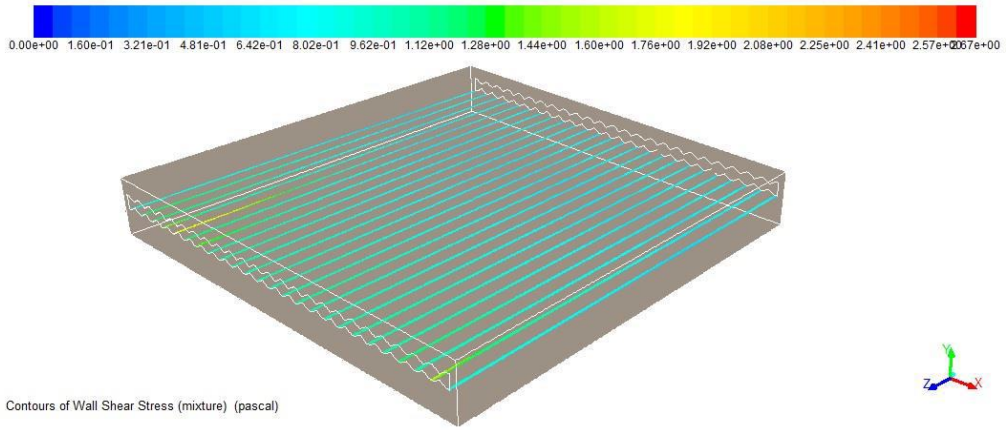

Fig. 11. Wall shear stress distribution on lower interface of a triangular fin micro-gap for $\Omega=2\times10^{-3}W$, $q_{in}=1\times10^{6}\ Wm^{-2}$, $\alpha_{in}=0$

4. Conclusions

Following key points are noted from this research: forexample:

i. Evaporation rate enhances with the increasing wall heat flux and decreases with the increasing pumping power. The decrement rate of evaporation slows down after achieving a threshold value of the pumping power.
ii. Wall shear stress rises with the increasing wall heat flux and pumping power and decreases with the decreasing inlet void fraction.

Acknowledgment

The support of Malaysian Ministry of Higher Education through International Islamic University Malaysia under the research grant FRGS19-126-0735 is gratefully acknowledged.

References

[1] Alam, Tamanna, Poh Seng Lee, Christopher R. Yap, and Liwen Jin. "Experimental investigation of microgap cooling technology for minimizing temperature gradient and mitigating hotspots in electronic devices." In *2011 IEEE 13th*

Electronics Packaging Technology Conference, pp. 530-535. IEEE, 2011. https://doi.org/10.1109/EPTC.2011.6184478

[2] Alam, Tamanna, Poh Seng Lee, Christopher R. Yap, and Liwen Jin. "A comparative study of flow boiling heat transfer and pressure drop characteristics in microgap and microchannel heat sink and an evaluation of microgap heat sink for hotspot mitigation." *International Journal of Heat and Mass Transfer* 58, no. 1-2 (2013): 335-347. https://doi.org/10.1016/j.ijheatmasstransfer.2012.11.020

[3] Ahmed, Shugata, Ahmad Faris Ismail, Erwin Sulaeman, and Muhammad Hasibul Hasan. "A critical assessment on evaporative cooling performance of micro finned micro gap for high heat flux applications." *ARPN Journal of Engineering and Applied Sciences* 11, no. 1 (2016): 313-336.

[4] Ahmed, Shugata, Muhammad Hasibul Hasan, Ahmad Faris Ismail, and Erwin Sulaeman. "Effect of geometrical parameters on boiling heat transfer and pressure drop in micro finned micro gap." *ARPN Journal of Engineering and Applied Sciences* 11, no. 1 (2016): 297-302.

[5] Ahmed, Shugata, Ahmad Faris Ismail, Erwin Sulaeman, and Muhammad Hasibul Hasan. "Study on turbulent characteristics of flow boiling in a micro gap under the influence of surface roughness and micro fins." *ARPN Journal of Engineering and Applied Sciences* 11, no. 1 (2016): 410-414.

[6] Ahmed, Shugata, Erwin Sulaeman, Ahmad Faris Ismail, and Muhammad Hasibul Hasan. "Two-Phase Fin-Induced Turbulent Cooling for Electronic Devices Using Heat Pump Associated Micro-Gap Heat Sink." *International Journal of Engineering & Technology* 3 (2018): 113-122. https://doi.org/10.14419/ijet.v7i3.13.16336

[7] Ahmed, Shugata, Ahmad Faris Ismail, Erwin Sulaeman, and Muhammad Hasibul Hasan. "Experimental Correlation for Flow-boiling Heat Transfer in a Micro-gap Evaporator with Internal Micro-fins." *Journal of Advanced Research in Fluid Mechanics and Thermal Sciences* 54, no. 1 (2019): 1-8.

[8] Ahmed, Shugata. "Study on fin-induced pseudo-turbulent flow boiling characteristics of micro-gap evaporators." (2017).

[9] Alam, Tamanna, Poh Seng Lee, Christopher R. Yap, and Liwen Jin. "Experimental investigation of local flow boiling heat transfer and pressure drop characteristics in microgap channel." *International Journal of Multiphase Flow* 42 (2012): 164-174. https://doi.org/10.1016/j.ijmultiphaseflow.2012.02.007

[10] Ahmed, Shugata, Ahmad Faris Ismail, Erwin Sulaeman, and Muhammad Hasibul Hasan. "A Comparative Analysis of Flow Boiling in Micro-Gaps with Internal Micro-Fins of Rectangular and Triangular Profiles." *International Journal of Applied Engineering Research* 11, no. 4 (2016): 2364-2372.

[11] Hirt, Cyril W., and Billy D. Nichols. "Volume of fluid (VOF) method for the dynamics of free boundaries." *Journal of computational physics* 39, no. 1 (1981): 201-225. https://doi.org/10.1016/0021-9991(81)90145-5

[12] Orszag, S. A., V. Yakhot, and W. S. Flanney. "Renormalization group modeling and turbulence, in international conference on near-wall turbulent flows." In *Proceedings of the International Symposium on Mathematical Modeling of Turbulent Flows. Tokyo, Japan*. 1995..

[13] Schrage, Robert W. *A theoretical study of interphase mass transfer*. Columbia University Press, 1953. https://doi.org/10.7312/schr90162

[14] Lee, Wen Ho. "A pressure iteration scheme for two-phase modeling." *Los Alamos Scientific Laboratory, Los Alamos, NM, Report No. LA-UR* (1979): 79-975.

[15] Wu, H. L., X. F. Peng, P. Ye, and Y. Eric Gong. "Simulation of refrigerant flow boiling in serpentine tubes." *International Journal of Heat and Mass Transfer* 50, no. 5-6 (2007): 1186-1195. https://doi.org/10.1016/j.ijheatmasstransfer.2006.10.013

[16] De Schepper, Sandra CK, Geraldine J. Heynderickx, and Guy B. Marin. "Modeling the evaporation of a hydrocarbon feedstock in the convection section of a steam cracker." *Computers & Chemical Engineering* 33, no. 1 (2009): 122-132. https://doi.org/10.1016/j.compchemeng.2008.07.013

[17] Alizadehdakhel, Asghar, Masoud Rahimi, and Ammar Abdulaziz Alsairafi. "CFD modeling of flow and heat transfer in a thermosyphon." *International Communications in Heat and Mass Transfer* 37, no. 3 (2010): 312-318. https://doi.org/10.1016/j.icheatmasstransfer.2009.09.002